Supplementary Materials for

Physics-informed models of domain wall dynamics as a route for autonomous domain wall design via reinforcement learning

Supplementary S1 – XRD

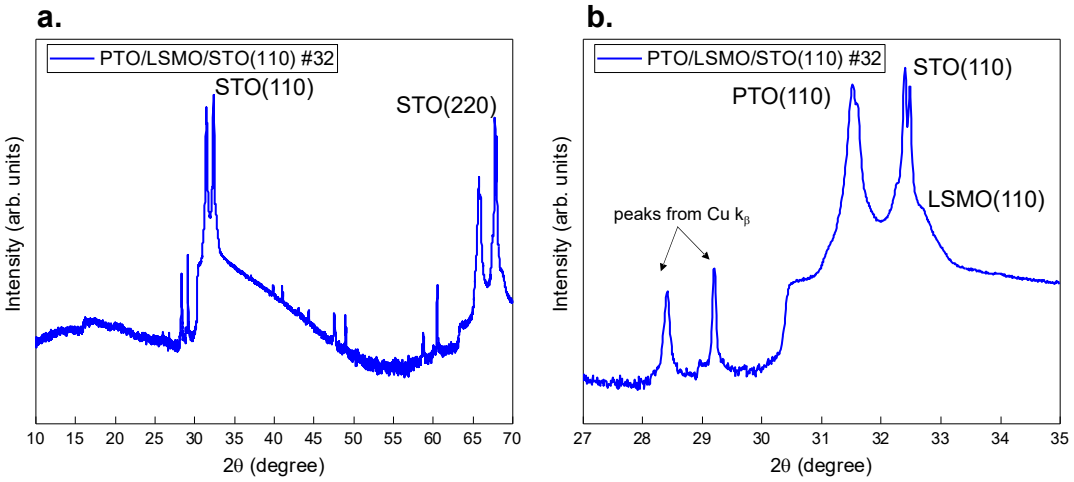

Figure S1: The θ-2θ x-ray diffraction (XRD) scans shown in a. and b. were acquired by using a Bruker D2 Phaser. (a) shows the θ-2θ scan from 10 to 70 degrees where features around STO (110) and STO (220) reflections are observed. The enlarged features near STO (110) reflection are presented in (b), where the diffraction from PTO (110) and LSMO (110) can be observed. The twin features of PTO (110) and STO (110) in the 2θ range of 31-33 degrees are contributed by the Cu Kα1 (λ=1.5406 Å) and Kα2 (λ=1.5444 Å) x-rays; while the extra peaks in the 2θ range of 28-30 degrees are produced by Cu Kβ (λ=1.3922 Å). The XRD suggests that only (110)-oriented PTO is present.

Supplementary S2 - Videos

The automated data collection was run on two separate days. The results from the first run (single frequency PFM) are shown in video "*data_1.mp4*" and the second round (which used band-excitation PFM) is shown in "*data_2.mp4*." Both are available at the links below:

https://www.dropbox.com/s/j5dqvgza3ugaff0/data_1.mp4?dl=0

https://www.dropbox.com/scl/fi/v3neofeva25p0hcs3wsia/data_2.mp4?rlkey=l9d01uk8g1i5my6vynekcjr7u&dl=0

Supplementary S3

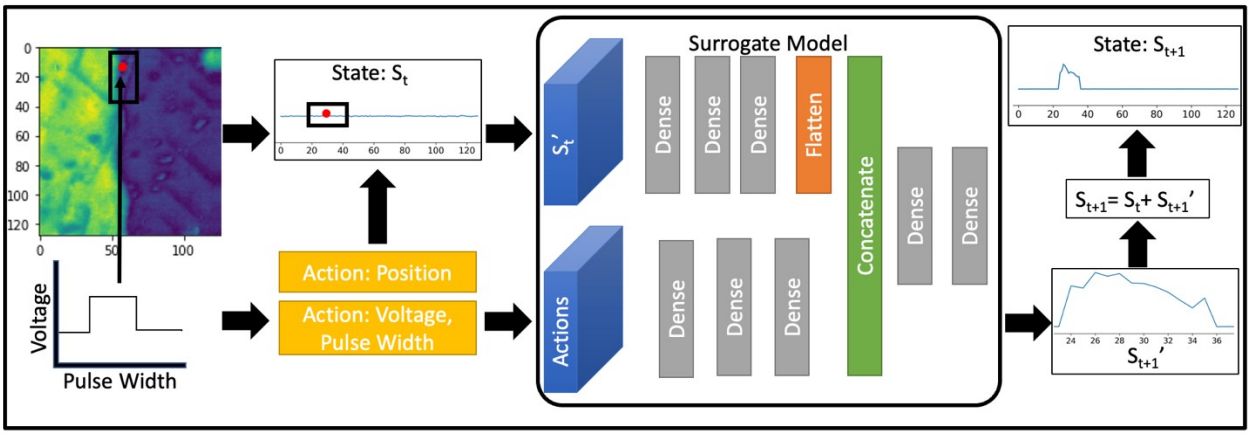

Figure S3: Architecture of the surrogate model. The surrogate model takes two inputs – the initial state of the domain wall (extracted from a PFM Image) as well as the action vector that describes the location, amplitude and pulse width of the bias pulse applied. It then outputs the change to the local wall structure which is added to the initial state vector to produce the result of the action.

Supplementary S4 – Performance on Test Dataset

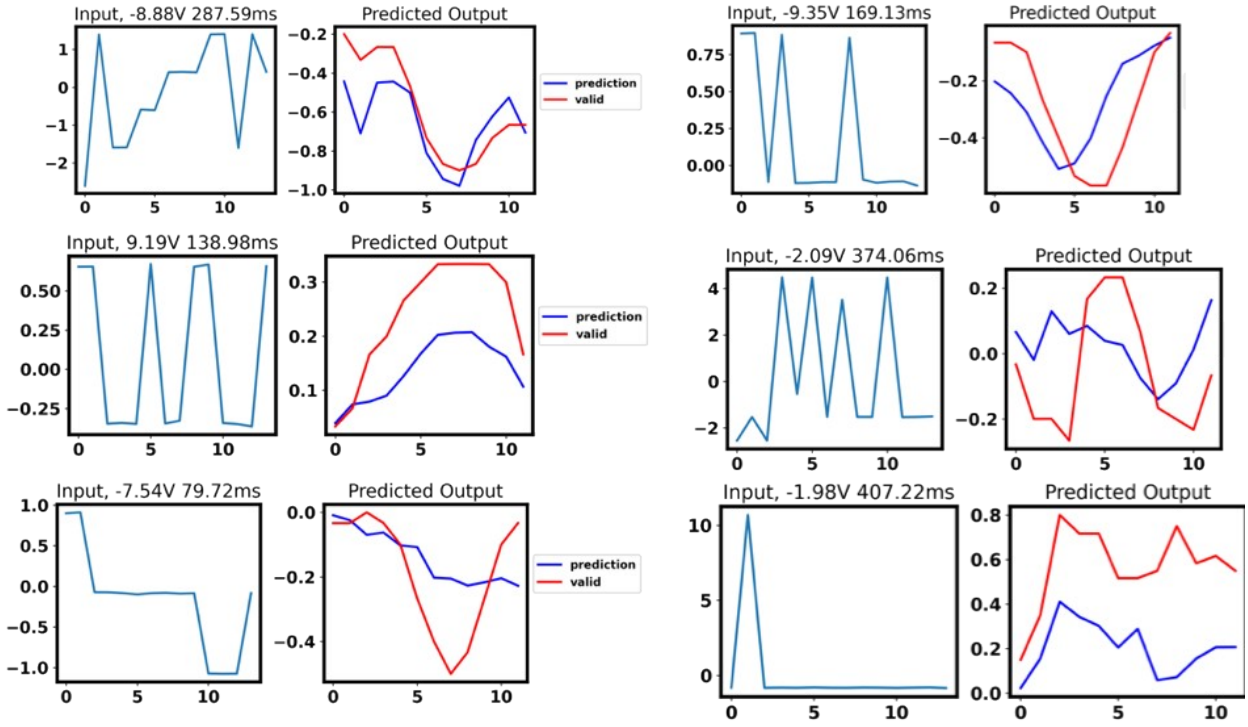

Figure S4: Performance on test dataset. Several examples of the testing of the surrogate model on held-out data are shown above. The input and output units are normalized. The mean absolute error on the test dataset is 13.2nm.

Supplementary S5 - Phase Field Simulations

In the phase field simulation, we used two coordinate systems: (i) $(\bar{1}\bar{1}0)$ oriented crystal coordinate system, and (ii) (001) oriented crystal coordinate system. We employed a polarization vector $P_i = (Px,Py,Pz)$ as the order parameter to represent the state of polarization in $(\bar{1}\bar{1}0)$ oriented coordinate system and $\acute{P}_j = (\acute{P}x,\acute{P}y,\acute{P}z)$ represent the state of polarization in (001) oriented coordinate system. To get the components of polarization in (001) oriented coordinate system, we used co-ordinate transformation from $(\bar{1}\bar{1}0)$ oriented coordinate system to (001) oriented coordinate system by using a transformation matrix A_{ij}, i.e., $\acute{P}_j = A_{ij}\, P_i$, where the transformation matrix A_{ij} is expressed as follows:

$$A_{ij} = \begin{bmatrix} 0 & 0 & 1 \\ -\frac{1}{\sqrt{2}} & \frac{1}{\sqrt{2}} & 0 \\ \frac{1}{\sqrt{2}} & -\frac{1}{\sqrt{2}} & 0 \end{bmatrix} \quad (1)$$

The total free energy of the system is given by,

$$F = \int_V [f_{elas}(P_i,\varepsilon_{ij}) + f_{grad}(P_{i,j}) + f_{bulk}(P_i) + f_{elec}(P_i,E_i)]\, dV \quad (2)$$

Where f_{elas} is elastic energy, f_{grad} is gradient energy, f_{bulk} is bulk energy, f_{elec} is electrostatic energy, ε_{ij} is elastic strain, and E_i is an electric field. The details about these energies can be found in the reference.[1]

The temporal evolution of the order parameter P_i is calculated by minimizing the total free energy of the system with respect to the order parameter P_i and by solving the following equation,[2]

$$\frac{\partial P_i(x,t)}{\partial t} = -L\frac{\partial F}{\partial P_i(x,t)} \quad (i = 1, 2, 3) \quad (3)$$

where L is the coefficient related to the mobility of the domain wall, x is spatial position, and t is time.

The system size was chosen to be $128\Delta x \times 128\Delta y \times 32\Delta z$, where $\Delta x = \Delta y = \Delta z = 1nm$. The total thickness $(32\Delta z)$ of the sample can be broken down into three regions: $10\Delta z$ substrate, $20\Delta z$ PTO thin film, and $2\Delta z$ air space. The simulation was performed at room temperature (T=25°C). To apply electrical potential, the local probe tip is set as a point tip and placed at the position (x_0, y_0) on the top of the film, whereas the bottom of the film is grounded $(0V)$. The half-width at half-magnitude (HWHM) of the tip is set to be $5nm$.

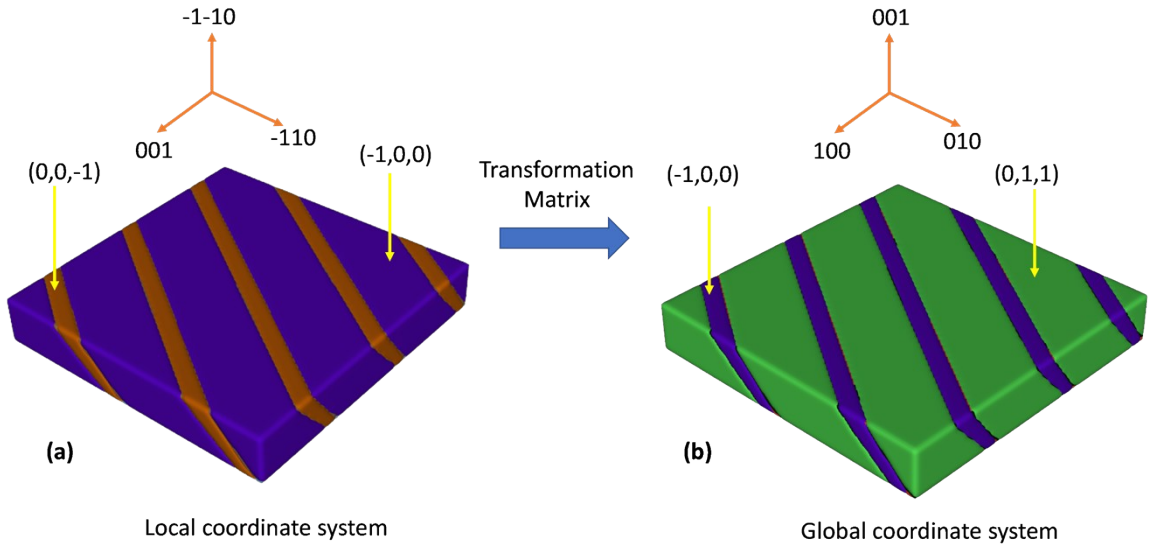

Figure S6. Equilibrium structure of the (110) oriented PTO thin film. **(a)** in a local coordinate system. **(b)** in a global coordinate system.

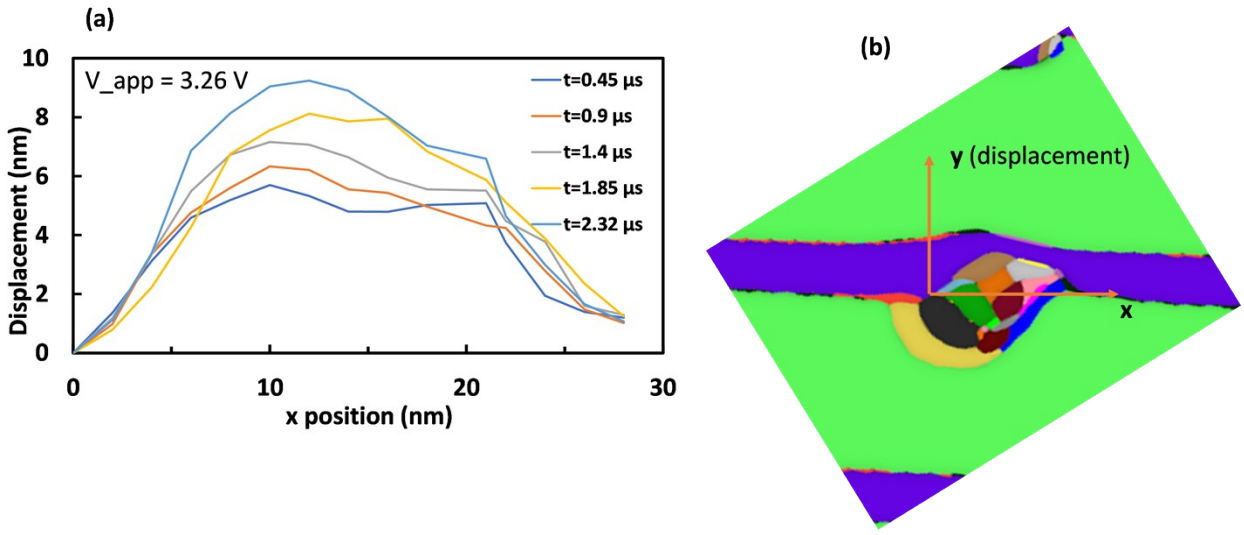

Figure S7. Wall displacement due to the applied bias. **(a)** wall displacement versus pulse width at bias 3.26 V. **(b)** coordinates system for the measurement of the wall displacement.

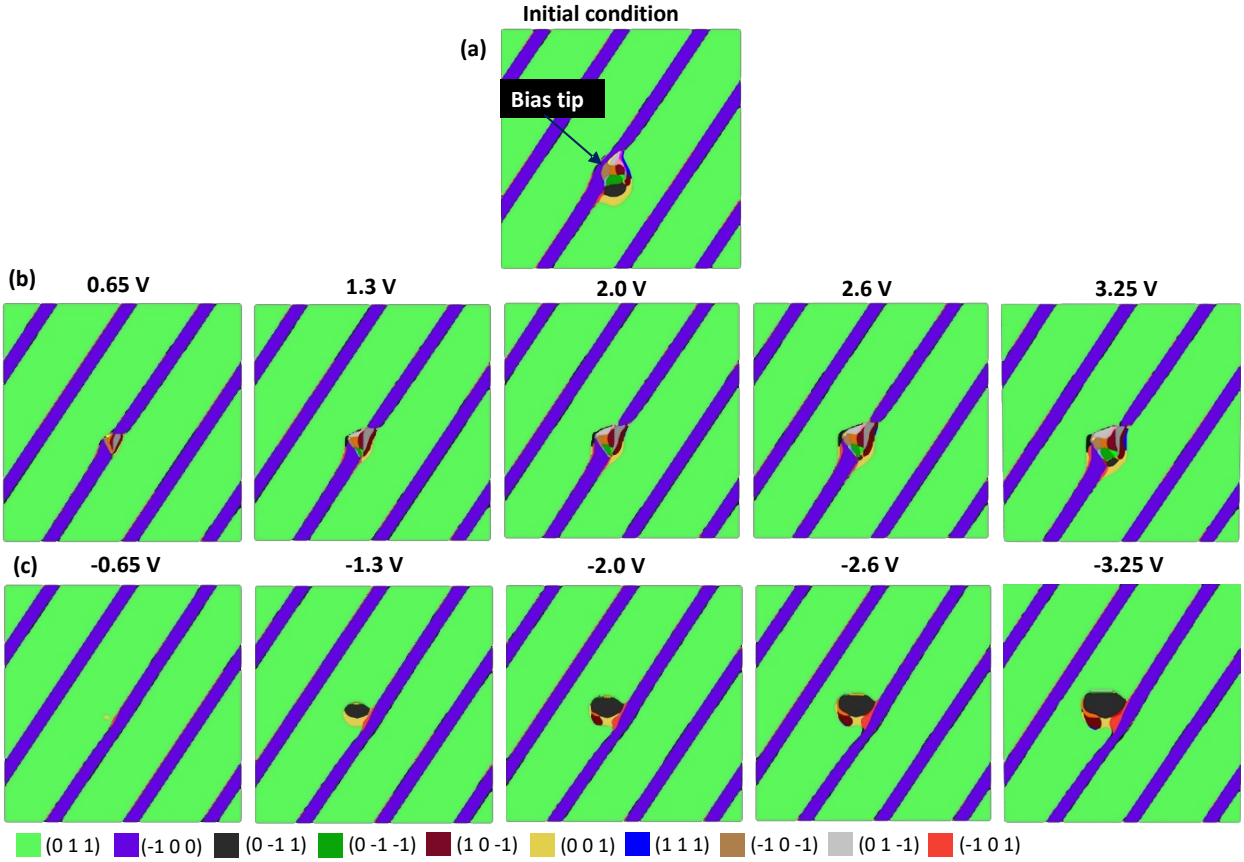

Figure S8. Response of the bulged wall to the different applied bias. **(a)** the initial condition of the bulged wall before applying the bias. The figure also shows the location where the bias tip

was placed. **(b)** wall displacement due to increasing positive bias. **(c)** wall displacement due to increasing negative bias.

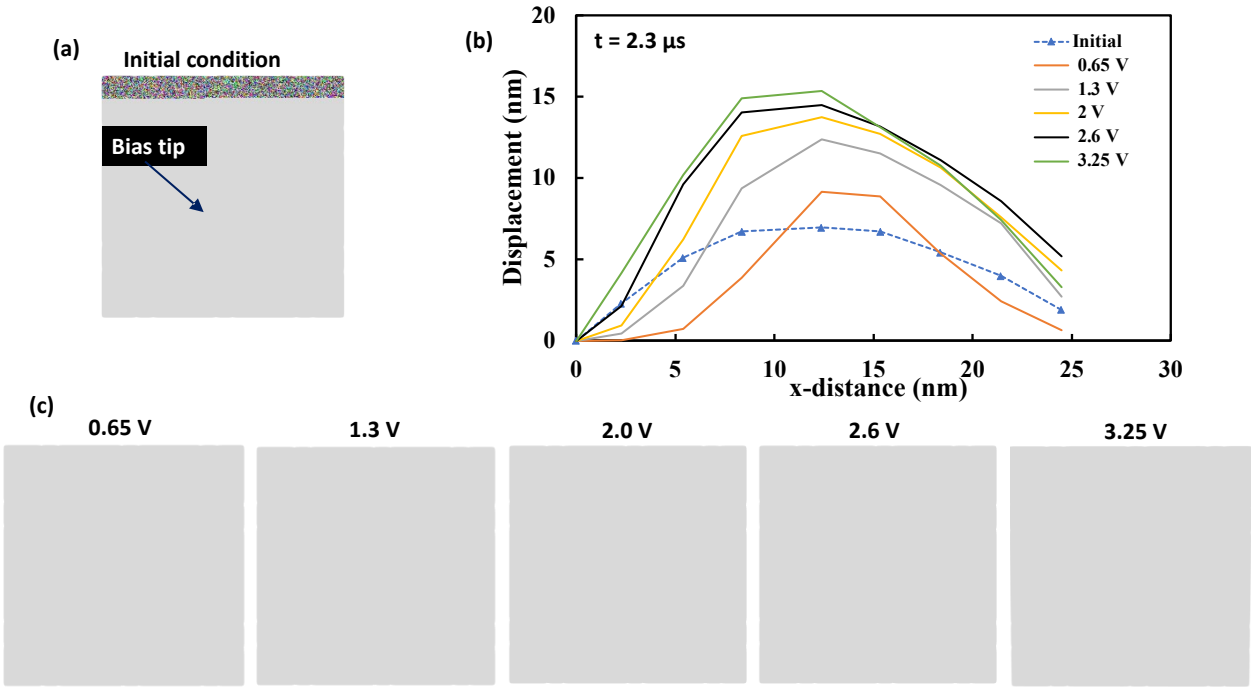

Figure S9: Applying positive bias to the already displaced ferroelastic domain wall. The initial condition is shown in (a) and the wall profile in (b), along with the effects of applying pulses of different voltages for a time of 2.3µs. The x-y map of the domain variants is shown in (c).

Python Code

There are two sections to the code. The first is the training of the dynamics model. This is included within the 'Dynamics model' folder, which includes the notebook that shows the preprocessing done to the original data ("*Dynamics Model_share.ipynb*"), and the training routines along with the use of the trained model and further analysis ("*dynamics model_Pre-trained.ipynb*"). The RL section describes the training and testing of the reinforcement learning policy. This is included in the notebook "*Rl_Walls_Trained_Final.ipynb*" in the "RL Code" folder.

References

1. H. Zhang, Y. P. Feng, Y. J. Wang, Y. L. Tang, Y. L. Zhu and X. L. Ma, *Acta Materialia*, 2022, **228**, 117761.
2. K. P. Kelley, Y. Ren, A. N. Morozovska, E. A. Eliseev, Y. Ehara, H. Funakubo, T. Giamarchi, N. Balke, R. K. Vasudevan, Y. Cao, S. Jesse and S. V. Kalinin, *ACS Nano*, 2020, **14**, 10569-10577.